Electronic Supplementary Information

Water Detection in Organic Solvents Using a Copolymer Membrane Immobilised with a Fluorescent Intramolecular Charge Transfer-Type Dye: Effects of Intramolecular Hydrogen Bonds

Ami Morimoto,[a] Kei Shimizu,[a] Naoya Suzuki,[a] Shigeyuki Yagi,[a] Kenji Sueyoshi,[a,b] Tatsuro Endo,[a] and Hideaki Hisamoto*[a]

[a] *Department of Applied Chemistry, Graduate School of Engineering, Osaka Metropolitan University, 1-1 Gakuen-cho, Naka-ku, Sakai, OSAKA, 599-8531 Japan*

[b] *CREST, Japan Science and Technology Agency*

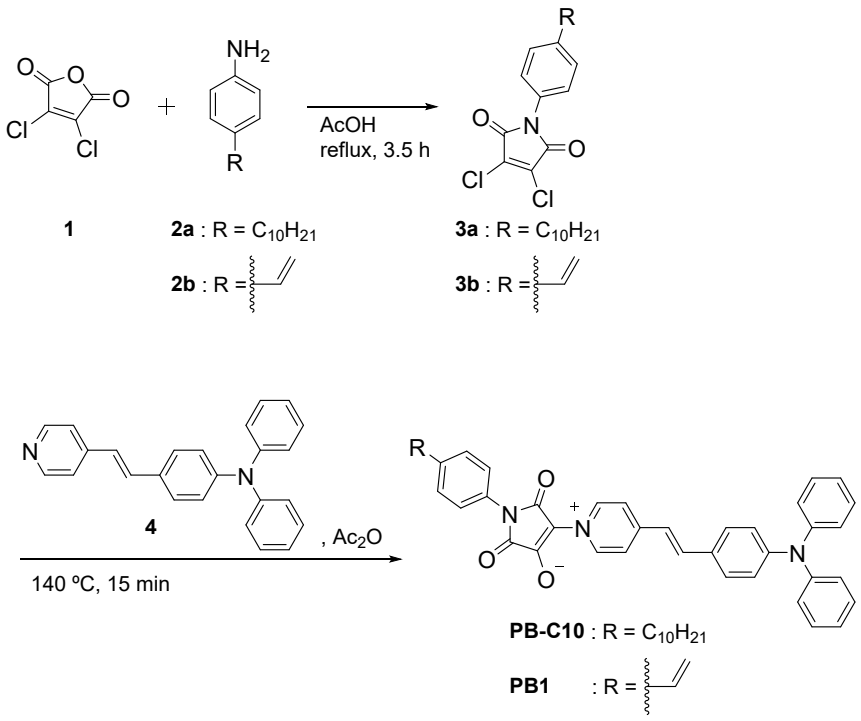

Scheme 1. Synthesis of pyridinium betaine dyes.

General

^{1}H NMR spectra (400 MHz) were obtained using a JEOL ECX-400 spectrometer with tetramethylsilane (0.00 ppm) as the internal standard. Low-resolution (LR) atmospheric solid analysis probe (ASAP) mass measurements were carried out with a Shimadzu LCMS-2020 and LabSolutions LCMS software. High-resolution (HR) electrospray ionization mass measurements were carried out with a Bruker microTOF system after calibration using a sodium formate solution. Elemental analyses were carried out on a J-Science Lab MICRO CORDER JM10 analyser. (*E*)-*N,N*-Diphenyl-4-(2-(pyridin-4-yl)vinyl)aniline (denoted as **4**) was synthesised according to a previously reported protocol.[1]

*Synthesis of **3a***

2,3-Dichloromaleic anhydride (0.4122 g, 2.469 mmol) and **2a** (0.5620 g, 2.408 mmol) were dissolved in acetic acid (5.0 mL), and the mixture was refluxed for 3.5 h. After cooling, water (10.0 mL) was added to the mixture, and the resulting precipitate was filtrated. The residue was washed with water and methanol, yielding the target compound **3a** as a white solid (0.8617 g, 2.254 mmol, 94 % yield); ^{1}H NMR (400 MHz, $CDCl_3$) δ 7.28 (d, J = 8.2 Hz, 2H), 7.22 (d, J = 8.2, 2H), 2.63 (t, J = 7.8 Hz, 2H), 1.66–1.58 (m, 2H), 1.31–1.26 (m, 14H), 0.88 (t, J = 6.9 Hz, 3H); ^{13}C NMR (100 MHz, $CDCl_3$) δ 162.3, 144.0, 133.7, 129.5, 128.1, 126.0, 35.8, 32.0, 31.4, 29.8, 29.7, 29.6, 29.5, 29.4, 22.8, 14.3; LR-ASAP-MS (*m*/*z*) calcd. For $C_{20}H_{26}Cl_2NO_2$ ($[M + H]^+$): 382.1; Found: 382.2; Anal. calcd. for $C_{20}H_{25}Cl_2NO_2$: C, 62.83; H, 6.59; N, 3.66. Found: C, 62.76; H, 6.54; N, 3.87.

*Synthesis of **3b***

2,3-Dichloromaleic anhydride (0.4593 g, 2.753 mmol) and **2b** (0.322 mL, 2.748 mmol) were dissolved in acetic acid (5.0 mL), and the mixture was refluxed for 3.5 h. After cooling, water (10.0 mL) was added to the mixture, and the resulting precipitate was filtrated. The residue was washed with water and methanol yielding the target compound **3a** as a white solid (0.6530 g, 2.436 mmol, 89 % yield); ^{1}H NMR (400 MHz, $CDCl_3$) δ 7.51 (d, *J* = 8.7 Hz, 2H), 7.31 (d, *J* = 8.7 Hz, 2H), 6.73 (dd, *J* = 17.4, 11.0 Hz, 1H, 5.79 (d, *J* = 17.4 Hz, 1H), 5.34 (d, *J* = 11.0 Hz, 1H); ^{13}C NMR (100 MHz, $CDCl_3$) δ 162.1, 138.1, 135.8, 133.8, 129.9, 127.2, 126.1, 115.7; LR-ASAP-MS (*m*/*z*) calcd. For $C_{12}H_7Cl_2NO_2$ ($[M + H]^+$): 268.0; Found: 268.0; Anal. calcd. for $C_{12}H_7Cl_2NO_2$: C, 53.76; H, 2.63; N, 5.22. Found: C, 53.63; H, 3.02; N, 5.19.

*Synthesis of **PB-C10***

The compounds **4** (98.0 mg, 0.2812 mmol), **3a** (116.5 mg, 0.3047 mmol), and acetic anhydride (3.0 mL) were mixed, and the blend was refluxed for 15 min and then cooled in an ice bath. The obtained precipitate was filtrated and then washed with methanol and ethanol, yielding the target compound **PB-C10** as a reddish-orange powder in 86% yield (0.1632 g, 0.2415 mmol); ^{1}H NMR (400 MHz, CD_2Cl_2) δ 9.66 (d, *J* = 7.3 Hz, 2H), 7.71 (d, *J* = 7.3 Hz, 2H), 7.49–7.45 (m, 3H), 7.33–7.25 (m, 8H), 7.40–7.12 (m, 6H), 7.00 (d, *J* = 8.7 Hz, 2H), 6.96 (d, *J* = 16.5 Hz, 1H), 2.63 (t, *J* = 7.8 Hz, 2H), 1.66–1.58 (m, 2H), 1.28–1.25 (m, 14H), 0.86 (t, *J* = 6.9 Hz, 3H); ^{13}C NMR (100 MHz, $CDCl_3$) δ 167.1, 165.0, 163.5, 150.3, 147.3, 146.7, 142.4, 138.8, 136.5, 129.7, 129.3, 129.1, 129.0, 127.6, 126.4, 125.7, 124.5, 122.3, 121.4, 119.9, 100.2, 35.7, 32.0, 31.5, 29.7, 29.7, 29.6, 29.4, 22.8, 14.2; ESI-TOF MS (*m*/*z*) calcd. For $C_{45}H_{45}N_3NaO_3$ ($[M + Na]^+$): 698.3354; Found: 698.3345; Anal. calcd. for $C_{45}H_{45}N_3O_3$: C, 79.97; H, 6.71; N, 6.22. Found: C, 79.79; H, 6.76; N, 6.12.

*Synthesis of **PB1***

The compounds **4** (26.0 mg, 74.6 μmol), **3b** (22.5 mg, 83.9 μmol), and acetic anhydride (0.5 mL) were mixed, and the blend was refluxed for 15 min and then cooled in an ice bath. Hexane (10.0 mL) was added to the mixture, and the resulting precipitate was filtrated. The residue was washed with methanol and ethanol, yielding the target compound **PB1** as a reddish-orange powder in 96.2% yield (40.3 mg, 71.8 μmol); ^{1}H NMR (400 MHz, CD_2Cl_2) δ 9.65 (d, *J* = 6.9 Hz, 2H), 7.71 (d, *J* = 6.9 Hz, 2H), 7.50–7.44 (m, 5H), 7.36–7.29 (m, 6H), 7.14–7.12 (m, 6H), 7.00 (d, *J* = 9.2 Hz, 2H), 6.96 (d, *J* = 16.0 Hz, 1H), 6.74 (dd, *J* = 18.1, 11.0 Hz, 1H), 5.78 (d, *J* = 18.1 Hz, 1H), 5.28 (d, *J* = 11.0 Hz, 1H); ^{13}C NMR (100 MHz, $CDCl_3$) δ 166.9, 164.9, 163.3, 150.4, 147.5, 146.7, 139.0, 136.7, 136.3, 131.2, 129.7, 129.3, 127.6, 126.8, 126.5, 125.8, 124.6, 122.3, 121.5, 119.9, 114.6, 100.3; ESI-TOF MS (*m*/*z*) calcd. For $C_{37}H_{27}N_3NaO_3$ ($[M + Na]^+$): 584.1945; Found: 584.1940; Anal. calcd. for $C_{37}H_{27}N_3O_3$: C, 79.13; H, 4.85; N, 7.48. Found: C, 79.01; H, 4.97; N, 7.36.

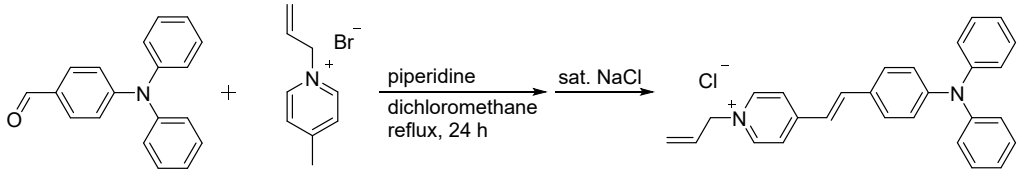

Scheme 2. Synthesis of **QP1**.

*Synthesis of **QP1***

QP1 was synthesised according to a previously reported method[2]. Briefly, the compound **5** (0.5940 g, 2.173 mmol) and **6** (0.4673 g, 2.182 mmol) were dissolved in dichloromethane (4.0 mL), and piperidine (20 μL, 0.20 mmol) was added to the mixture. The blend was refluxed for 24 h. After cooling, chloroform (30 mL) and water (30 mL) were added to the mixture, and the organic layer was washed with water (30 mL × 1) and sat. NaCl *aq*. (30 mL × 2) and dried over Na_2SO_4. Then, the solvent was removed on a rotary evaporator, and the residue was purified by silica gel column chromatography (eluent: chloroform/methanol = 4/1 (v/v)). The target compound **QP1** was obtained as a red solid (0.3110 g, 0.7318 mmol, 34% yield) ; ^{1}H NMR (400 MHz, $CDCl_3$) δ 9.12 (d, J = 6.4 Hz, 2H), 7.89 (d, J = 6.9 Hz, 2H), 7.61 (d, J = 16.0 Hz, 1H), 7.46 (d, J = 8.7 Hz, 2H), 7.35–7.31 (m, 4H), 7.16–7.13 (m, 6H), 7.01 (d, J = 8.7 Hz, 2H), 6.95 (d, J = 16.0 Hz, 1H), 6.17–6.07 (m, 1H), 5.58–5.49 (m, 4H); ^{13}C NMR (100 MHz, $CDCl_3$) δ 154.0, 150.7, 146.5, 144.1, 142.1, 130.8, 130.0, 129.7, 127.2, 125.9, 124.7, 123.5, 123.3, 121.0, 119.2, 62.1; ESI-TOF MS (*m*/*z*) calcd. For $C_{28}H_{25}N_2$ ($[M]^+$): 389.2013; Found: 389.2003; Anal. calcd. for $C_{28}H_{25}ClN_2$: C, 79.14; H, 5.93; N, 6.59. Found: C, 78.90; H, 5.99; N, 6.46.

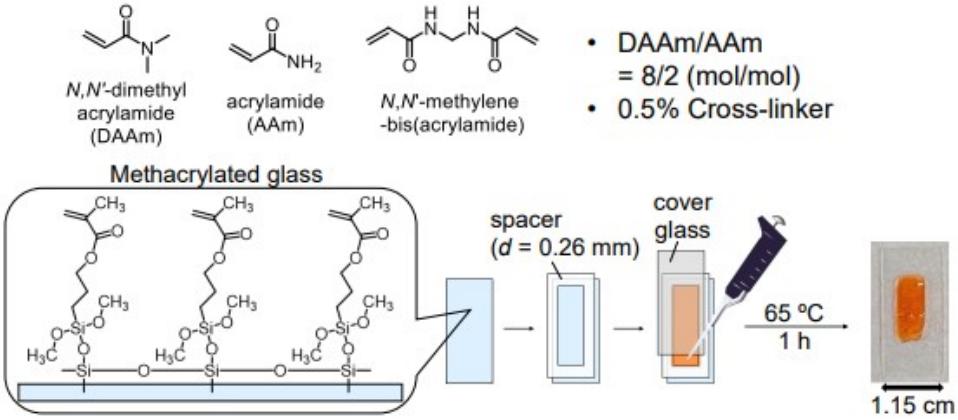

Fig. S1. Preparation of the dye-immobilised copolymer membrane.

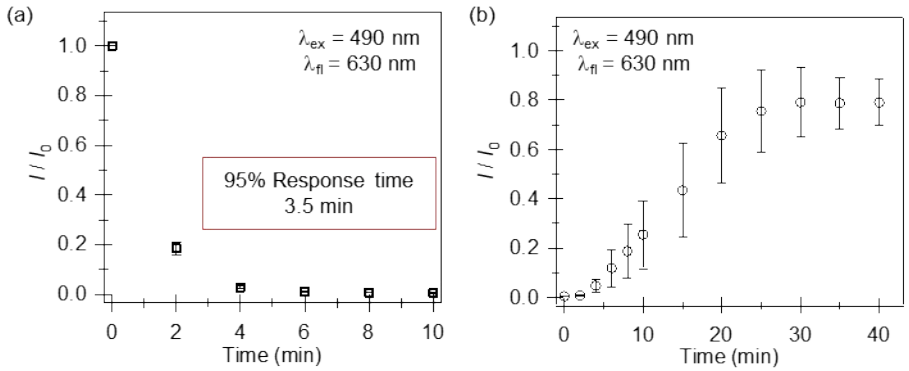

Fig. S2. (a) Response of the fluorescence intensity of **PB1**-mem to water in THF/water mixtures (from 0 vol% water in THF at 0 min to 40% water in THF). (b) Recovery of the fluorescence intensity of **PB1**-mem (from 40 vol% water in THF at 0 min to 0% water in THF).

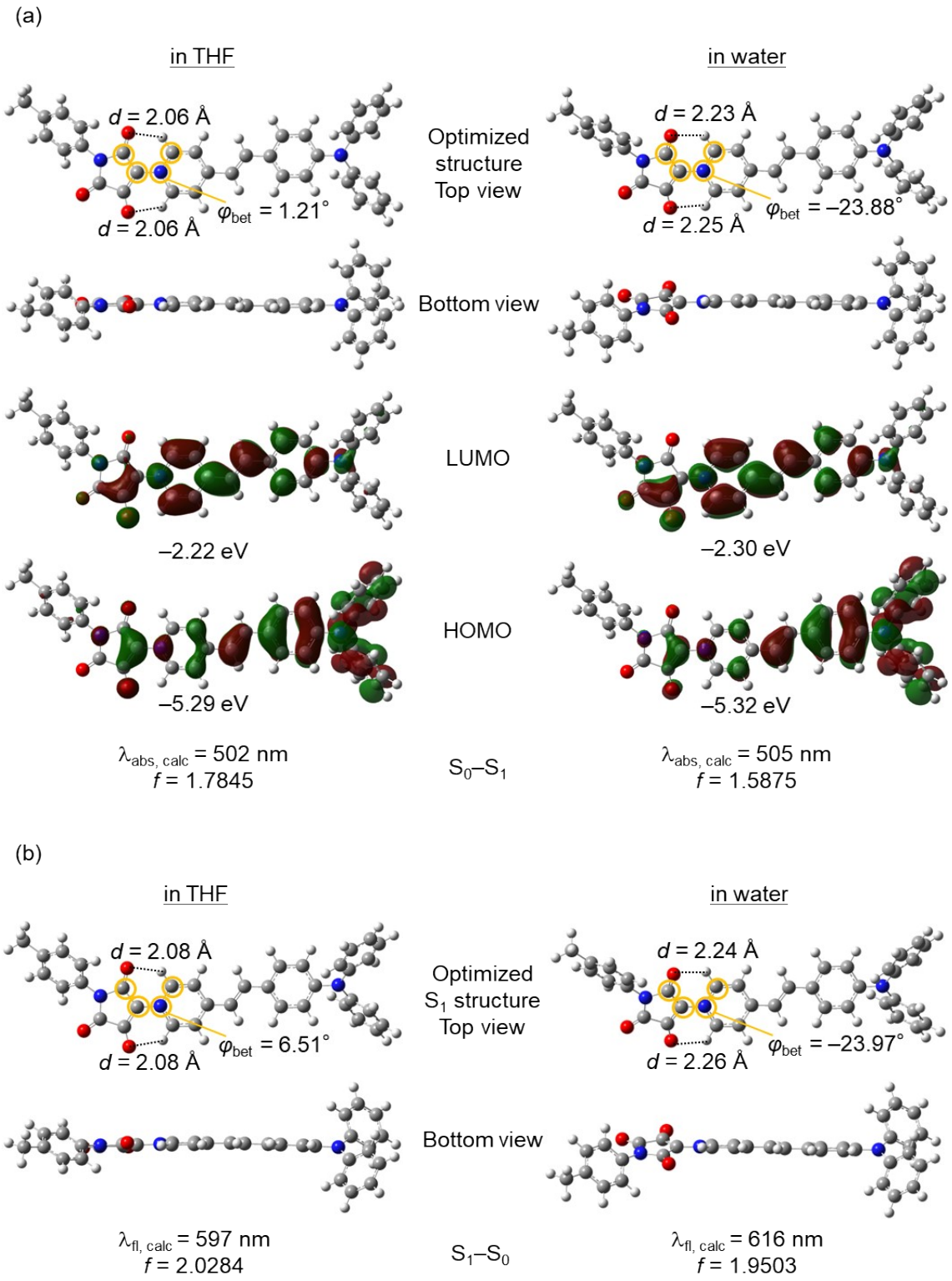

Fig. S3. (a) Optimized structures and the distribution of frontier orbitals in the ground state and (b) optimized structures in the excited state of **PB1** (left: SMD/THF, right: SMD/water at M06/6-31G(d,p) level).

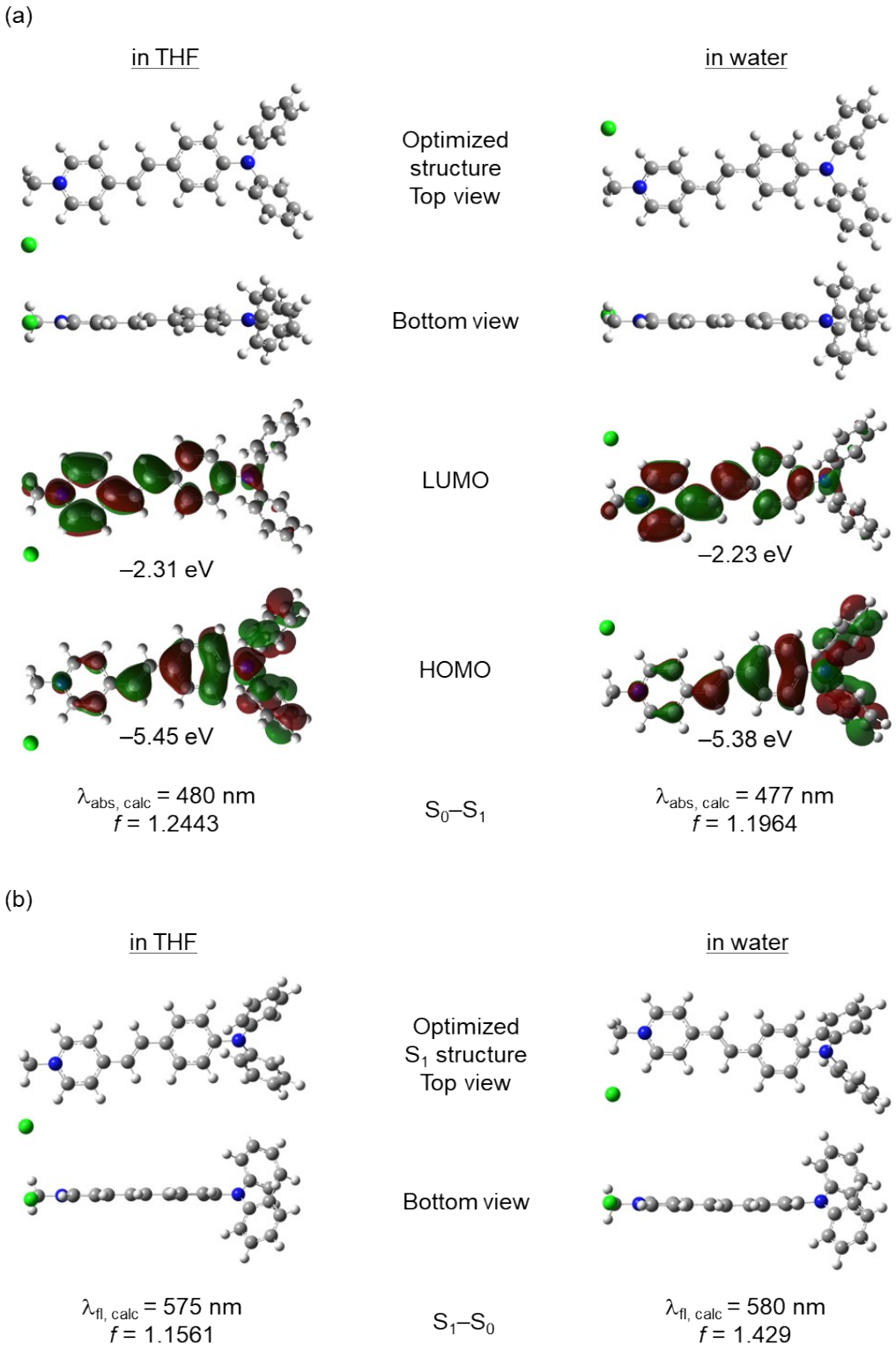

Fig. S4. (a) Optimized structures in the ground state and frontier orbitals and (b) optimized structure in the excited state of **QP1** (left: SMD/THF, right: SMD/water at M06/6-31G(d,p) level).

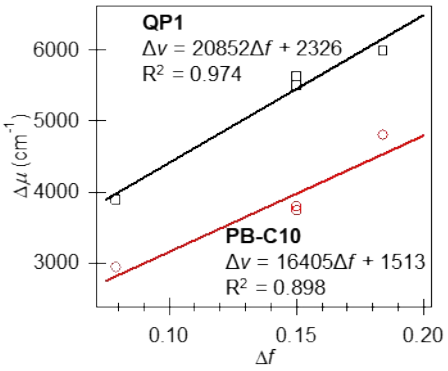

$$\bar{\nu}_g - \bar{\nu}_e = \frac{2}{hc}\frac{(\mu_e - \mu_g)^2}{a^3}\Delta f + constant$$

$$\Delta f = \left(\frac{\varepsilon - 1}{2\varepsilon + 1} - \frac{n^2 - 1}{2n^2 + 1}\right)$$

$(\bar{\nu}_g - \bar{\nu}_e)$: Stokes shifts (cm^{-1})
h : Planck's constant (6.6256×10^{-2} ergs)
c : speed of light (2.9979×10^{10} cm/s)
ε : dielectric constant of solvent
n : refractive index of solvent
μ_g, μ_e : dipole moment in the ground and excited state
a : radius of the cavity of the solute molecule

Fig. S5. Lippert–Mataga plots of the two synthesised dyes.

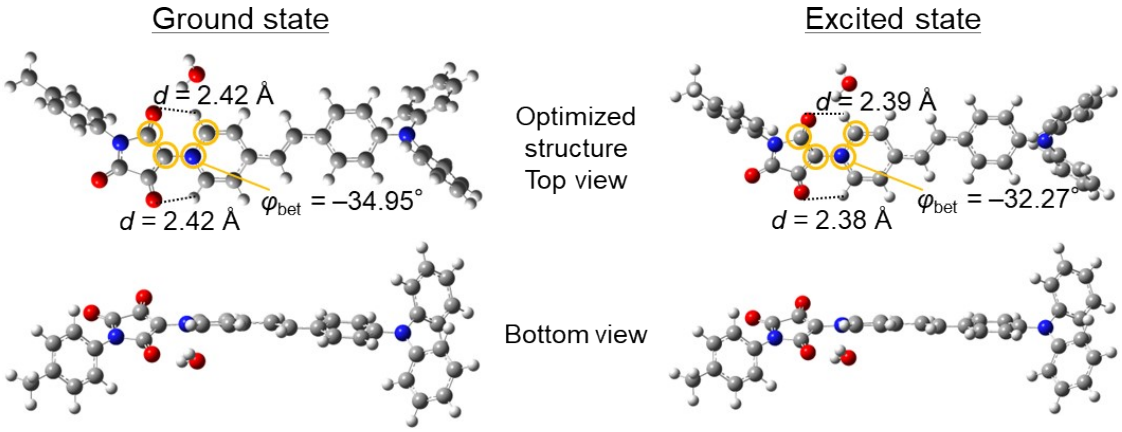

Fig. S6. Optimized structures in the ground state and excited states of **PB1** with a water molecule (SMD/water at M06/6-31G(d,p) level).

Table S1. Total energy of **PB1** and water in the ground state (SMD/water at M06/6-31G(d,p) level).

Optimized structure	Total energy (a.u.)
PB1 (Fig. S3a)	–1776.837859
Water	–76.39901008
PB1 + water (Fig. S6)	–1853.244426
$\Delta E_{total,g}$	0.00755732 (4.742294 kcal/mol)

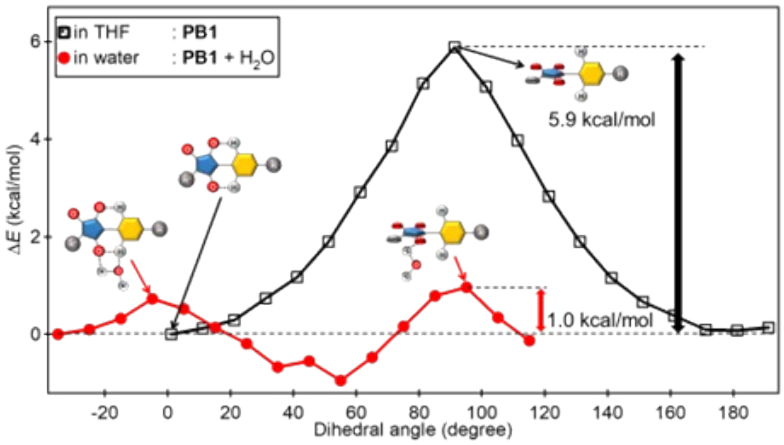

Fig. S7. Rotational energy barrier ΔE_g plotted against the dihedral angle $\varphi_{bet,g}$ between the maleimide and pyridinium rings (C–C–N–C) in the ground state.

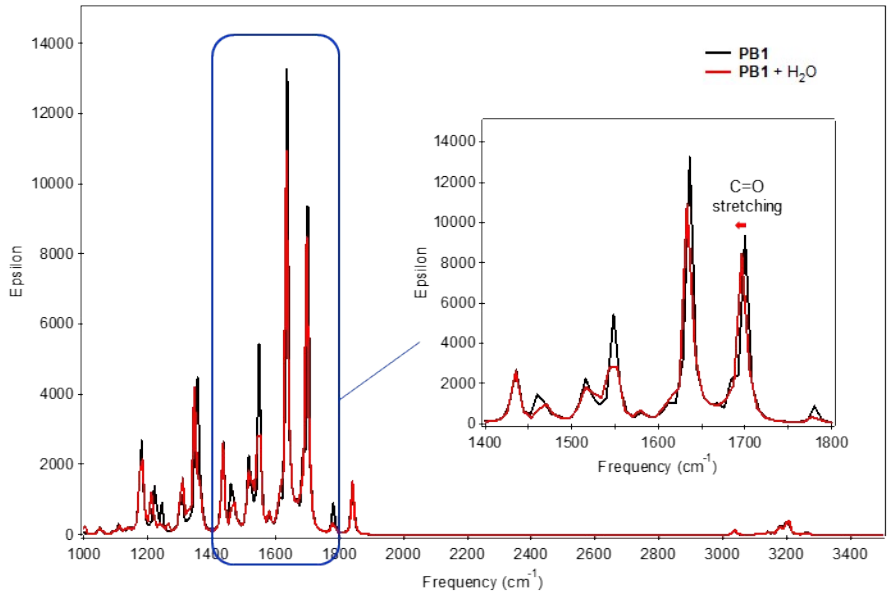

Fig. S8. Predicted IR spectra of **PB1** (SMD/water).

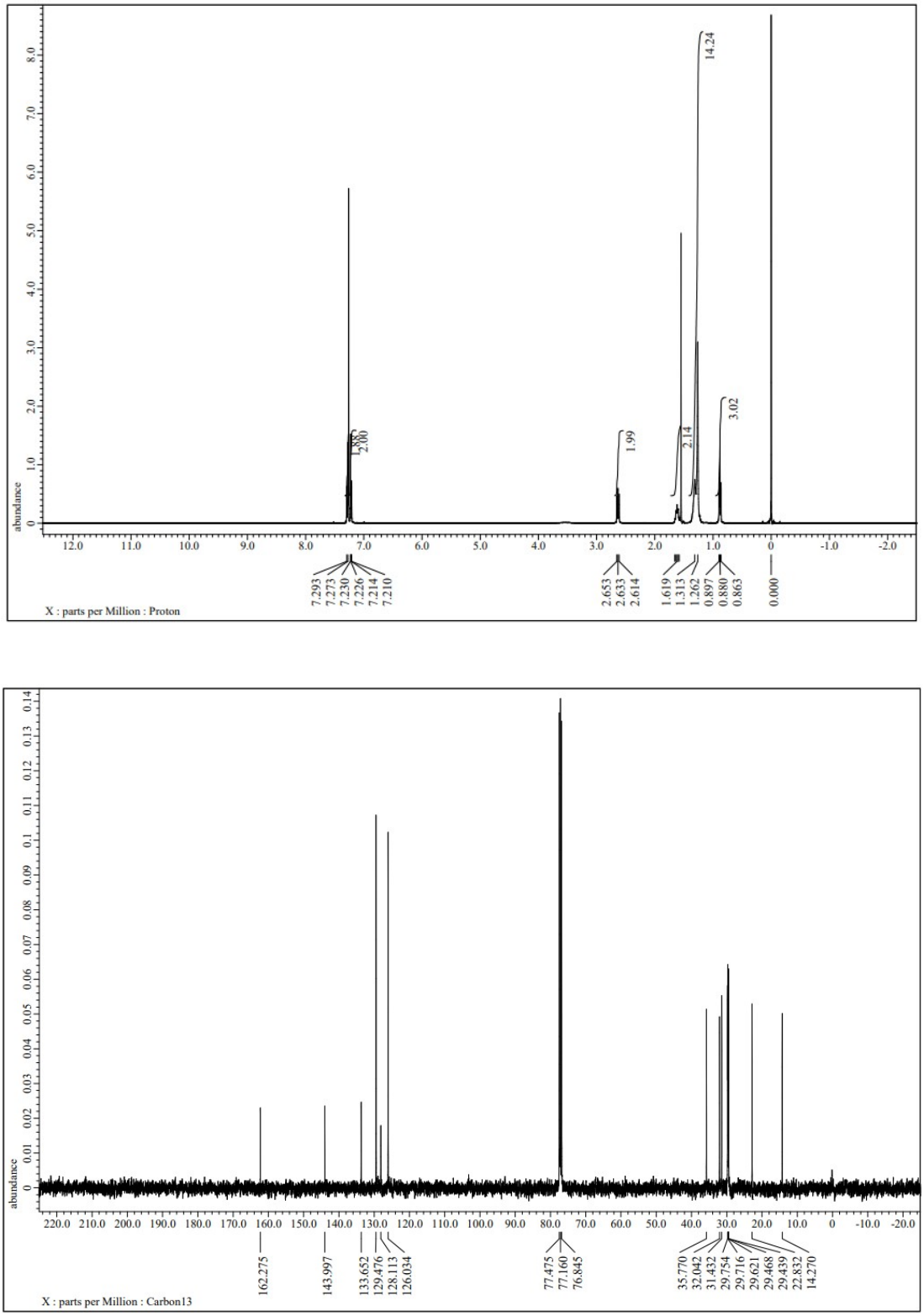

Fig. S9. ^{1}H NMR (above) and ^{13}C NMR (below) spectra of **3a** in $CDCl_3$.

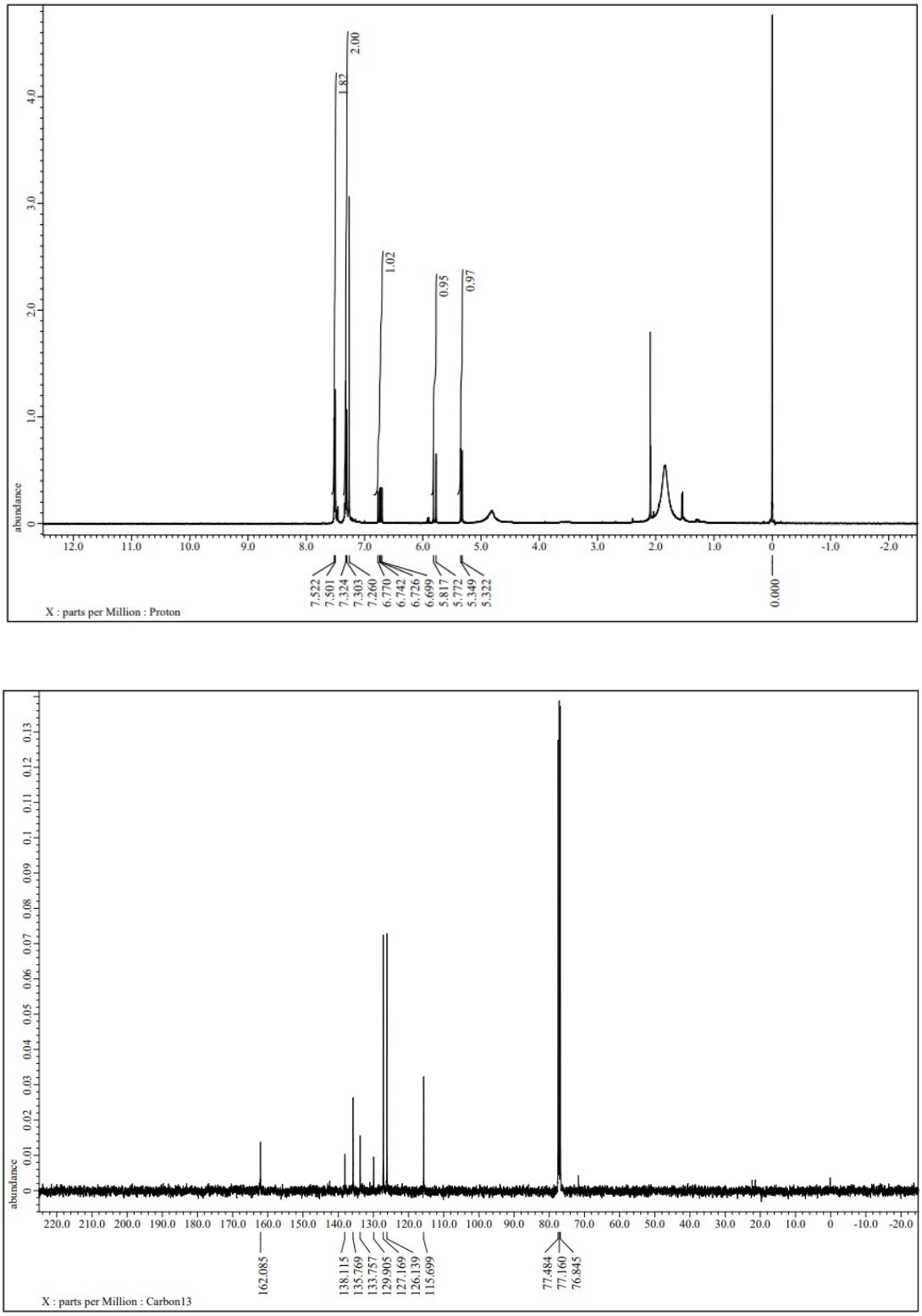

Fig. S10. ^{1}H NMR (above) and ^{13}C NMR (below) spectra of **3b** in $CDCl_3$.

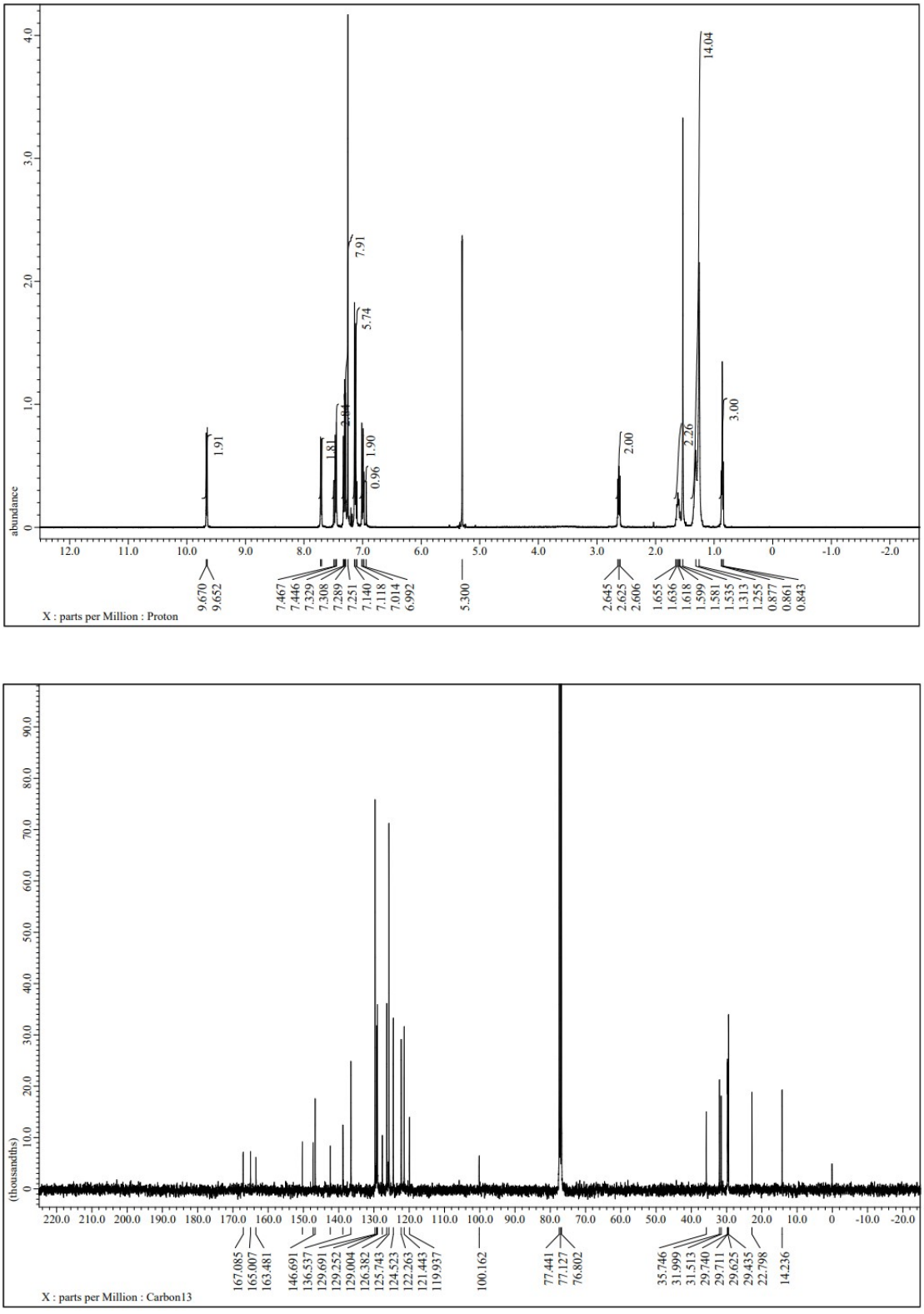

Fig. S11. ^{1}H NMR spectrum in CD_2Cl_2 (above) and ^{13}C NMR spectrum in $CDCl_3$ (below) of **PB-C10**.

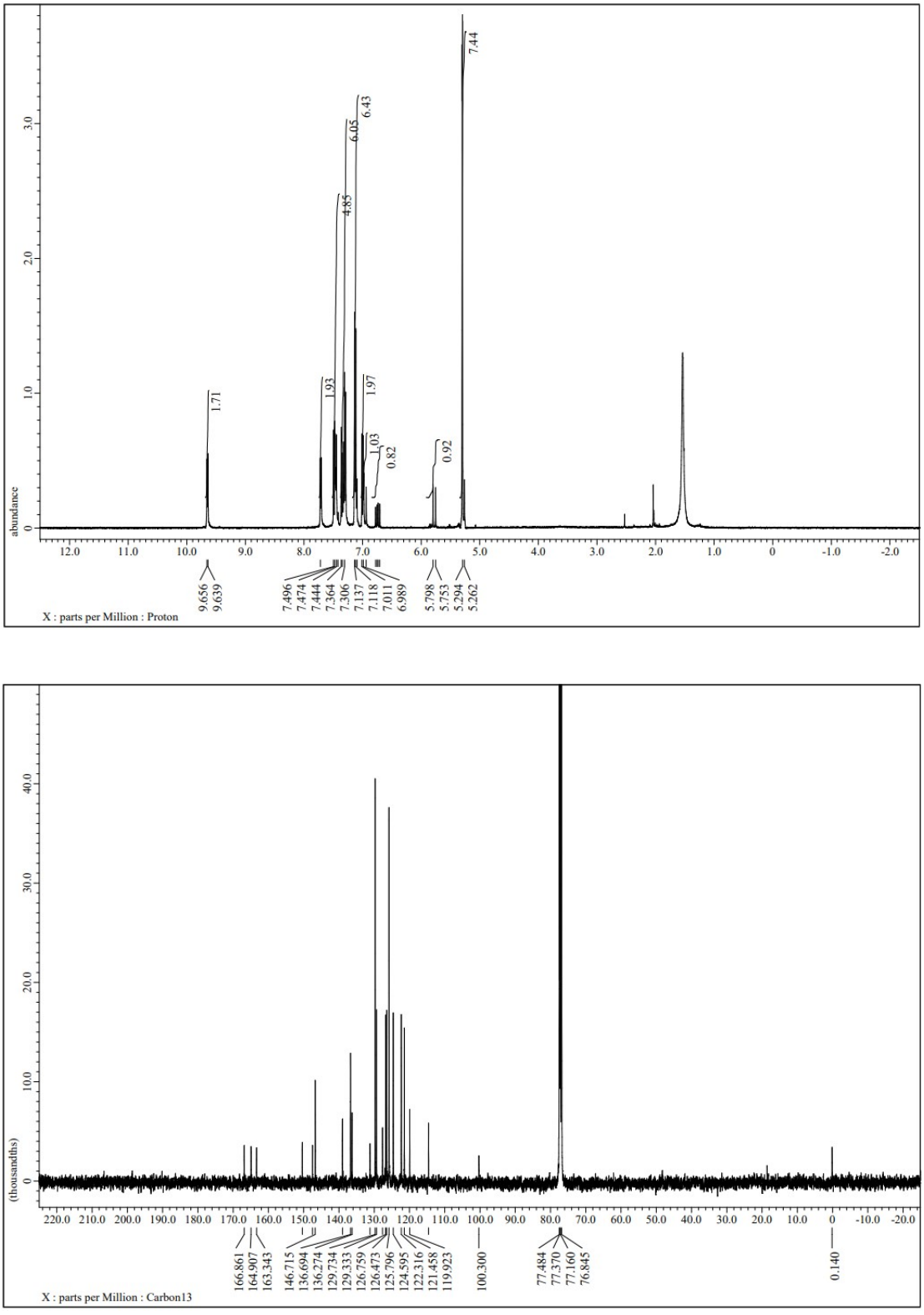

Fig. S12. ^{1}H NMR spectrum in CD_2Cl_2 (above) and ^{13}C NMR spectrum in $CDCl_3$ (below) of **PB1**.

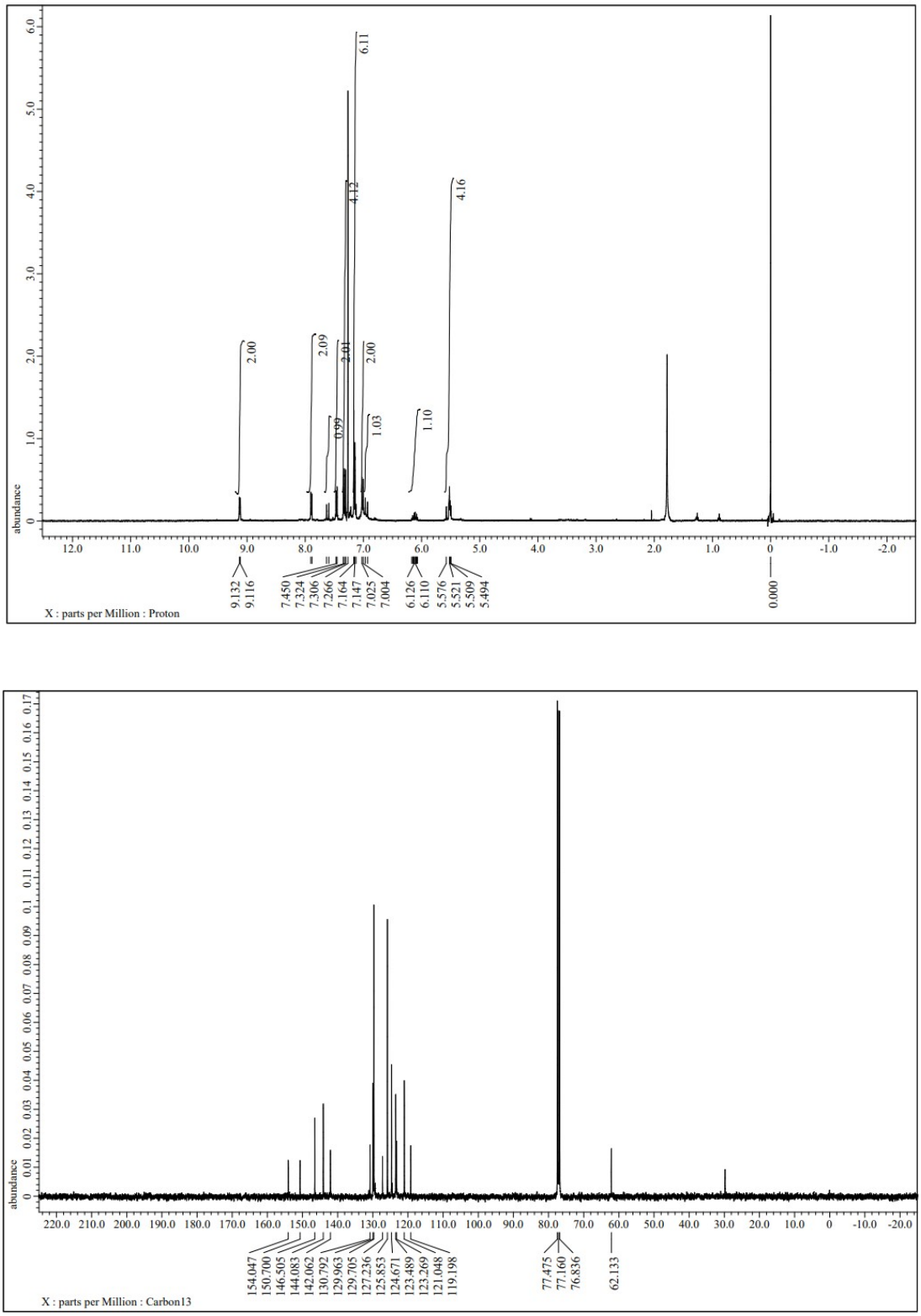

Fig. S13. ^{1}H NMR (above) and ^{13}C NMR (below) spectra of **QP1** in $CDCl_3$.

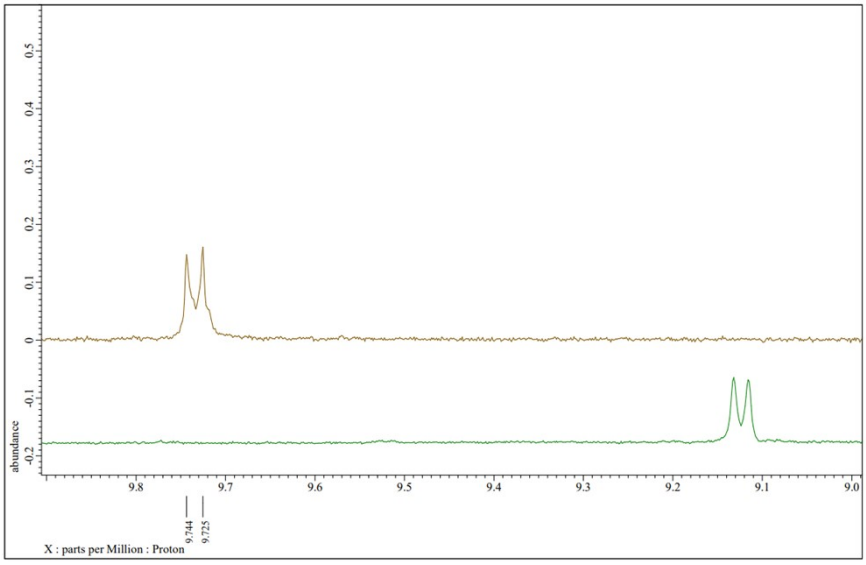

Fig. S14. ^{1}H NMR spectra of α-hydrogens of the pyridinium ring (brown line: **PB1**, green line: **QP1**, in $CDCl_3$).

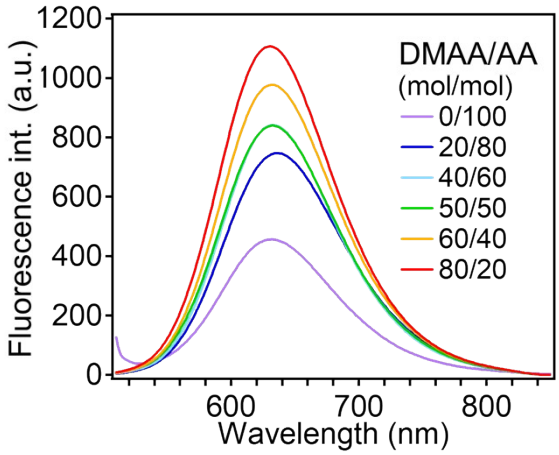

Fig. S15. Fluorescence spectra of **PB1**-mem with each ratio of DMAA/AAm (mol/mol) in anhydrous THF (λ_{ex} = 490 nm).

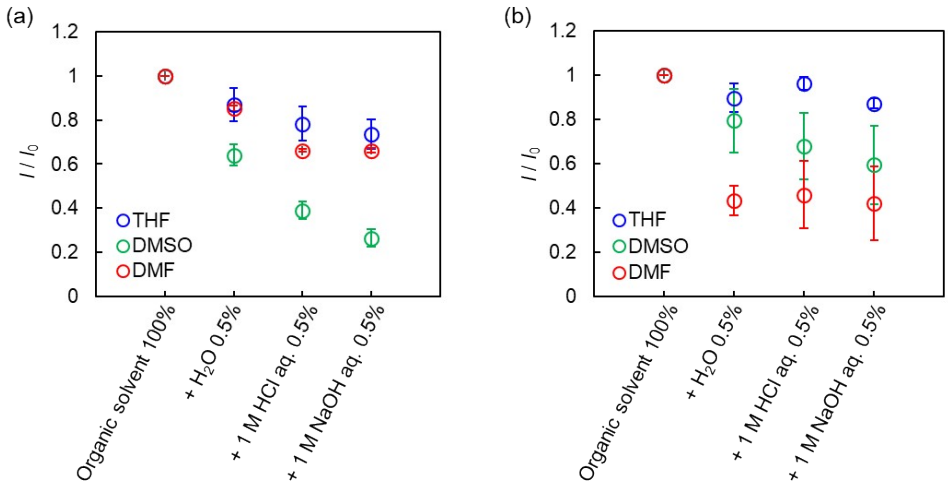

Fig. S16. Effects of acid (1M HCl aq.) and base (1M NaOH aq.) as impurities in THF, DMSO, and *N*,*N*-dimethylformamide (DMF). (a) **PB1**-mem (λ_{ex} = 490 nm) and (b) **QP1**-mem (λ_{ex} = 460 nm) in each solution. Each impurity was 0.5 vol% added to each organic solvents, and the membranes were soaked in each solution for 5 minutes. Then, fluorescence spectra were measured, and relative fluorescence intensity to that in an anhydrous organic solvent was investigated.

References

(1) He, X.; Yang, Y.; Guo, Y.; Lu, S.; Du, Y.; Li, J. J.; Zhang, X.; Leung, N. L. C.; Zhao, Z.; Niu, G.; et al. Phage-Guided Targeting, Discriminative Imaging, and Synergistic Killing of Bacteria by AIE Bioconjugates. *J. Am. Chem. Soc.* **2020**, *142* (8), 3959–3969. DOI: 10.1021/jacs.9b12936

(2) Kang, M.; Zhou, C.; Wu, S.; Yu, B.; Zhang, Z.; Song, N.; Lee, M. M. S.; Xu, W.; Xu, F.-J.; Wang, D.; et al. Evaluation of Structure–Function Relationships of Aggregation-Induced Emission Luminogens for Simultaneous Dual Applications of Specific Discrimination and Efficient Photodynamic Killing of Gram-Positive Bacteria. *J. Am. Chem. Soc.* **2019**, *141* (42), 16781–16789. DOI: 10.1021/jacs.9b07162